nature medicine

Periostin induces proliferation of differentiated cardiomyocytes and promotes cardiac repair

Bernhard Kühn[1], Federica del Monte[2], Roger J Hajjar[2,4], Yuh-Shin Chang[3], Djamel Lebeche[2,4], Shima Arab[1] & Mark T Keating[1,4]

Adult mammalian hearts respond to injury with scar formation and not with cardiomyocyte proliferation, the cellular basis of regeneration. Although cardiogenic progenitor cells may maintain myocardial turnover, they do not give rise to a robust regenerative response. Here we show that extracellular periostin induced reentry of differentiated mammalian cardiomyocytes into the cell cycle. Periostin stimulated mononucleated cardiomyocytes to go through the full mitotic cell cycle. Periostin activated α_V, β_1, β_3 and β_5 integrins located in the cardiomyocyte cell membrane. Activation of phosphatidylinositol-3-OH kinase was required for periostin-induced reentry of cardiomyocytes into the cell cycle and was sufficient for cell-cycle reentry in the absence of periostin. After myocardial infarction, periostin-induced cardiomyocyte cell-cycle reentry and mitosis were associated with improved ventricular remodeling and myocardial function, reduced fibrosis and infarct size, and increased angiogenesis. Thus, periostin and the pathway that it regulates may provide a target for innovative strategies to treat heart failure.

Differentiated cardiomyocytes carry the pump function of the heart. Loss of cardiomyocytes, which occurs, for example, after a large myocardial infarction, typically results in heart failure. Observations spanning the twentieth century show that some cardiomyocytes in the adult heart undergo DNA synthesis and mitosis[1,2]. Cell-cycle activity in the region bordering a myocardial infarction transiently increases tenfold to 0.004% (ref. 1). Although this increase is not sufficient for regeneration, it suggests that some cardiomyocytes have the potential to reenter the cell cycle in response to extracellular signals in the infarct border zone. It may be possible to apply specific extracellular factors to induce cardiomyocyte proliferation with the aim of enhancing cardiac regeneration.

In contrast to most adult cardiomyocytes, fetal cardiomyocytes do proliferate. After birth, cardiomyocytes become binucleated, downregulate cell-cycle activators, upregulate cell-cycle inhibitors, and withdraw from the cell cycle[3]. Although modification of intrinsic cell-cycle regulation can increase cell-cycle activity of differentiated cardiomyocytes[4–7], few extrinsic factors that induce cardiomyocyte proliferation are known.

Periostin comprises a signal peptide and four fasciclin-1 (fas1) domains. Alternative splicing of the carboxy terminus gives rise to periostin-like factor. Periostin, a component of the extracellular matrix[8], is associated with epithelial-mesenchymal transition during cardiac development[9,10]. Periostin is reexpressed in adult life after myocardial[11,12], vascular[13] and skeletal muscle[14] injury and after bone fracture[15]. Adenoviral gene delivery of periostin-like factor causes hypertrophic cardiomyopathy[16]. By contrast, liposomal gene delivery of periostin leads to dilative cardiomyopathy without hypertrophy[17].

Here we have investigated whether recombinant periostin, delivered through the cardiac extracellular matrix, can increase cardiomyocyte proliferation. We show that periostin induced reentry of differentiated mononucleated cardiomyocytes into the cell cycle. Periostin-induced cardiomyocyte cell-cycle reentry required integrins and the phosphatidylinositol-3-OH kinase (PI3K) pathway. After experimental myocardial infarction, periostin reduced infarct size and fibrosis and improved cardiac function. These results suggest that periostin treatment may enhance the regenerative capacity of adult mammalian hearts.

RESULTS

Periostin induces cycling of differentiated cardiomyocytes

The presence of periostin in the developing myocardium[9] and its ability to induce proliferation of neonatal cardiomyocytes (**Supplementary Fig. 1** online) prompted us to investigate whether periostin can induce cell cycle reentry of differentiated cardiomyocytes. Isolated adult rat ventricular cardiomyocytes with the characteristic rod shape (**Fig. 1a,b**) provided an *in vitro* assay platform. Recombinant human periostin[18] (500 ng/ml) was added for 9 d. After labeling with 5-bromodeoxyuridine (BrdU) for the last 3 d, DNA synthesis was determined. Tracking the fate of individual rod-shaped cardiomyocytes showed that they undergo DNA synthesis while expressing the cardiac contractile protein tropomyosin (**Fig. 1a**). Periostin induced a 14-fold

[1]Department of Cardiology, Children's Hospital Boston, 300 Longwood Avenue, Boston, Massachusetts 02115, USA. [2]Cardiovascular Research Center, Massachusetts General Hospital, 149 13th Street, Charlestown, Massachusetts 02129, USA. [3]Cardiovascular Research Center, Massachusetts General Hospital, 185 Cambridge Street, Boston, Massachusetts 02114, USA). [4]Present addresses: Cardiovascular Research Center, Mount Sinai School of Medicine, One Gustave Levy Place, New York, New York 10029, USA (R.J.H., D.L.); Novartis Institutes for BioMedical Research, Inc., 500 Technology Square, Cambridge, Massachusetts 02139, USA (M.T.K.). Correspondence should be addressed to B.K. (bernhard.kuhn@cardio.chboston.org) or M.T.K. (mark.keating@novartis.com).

Received 13 January; accepted 13 June; published online 15 July 2007; doi:10.1038/nm1619

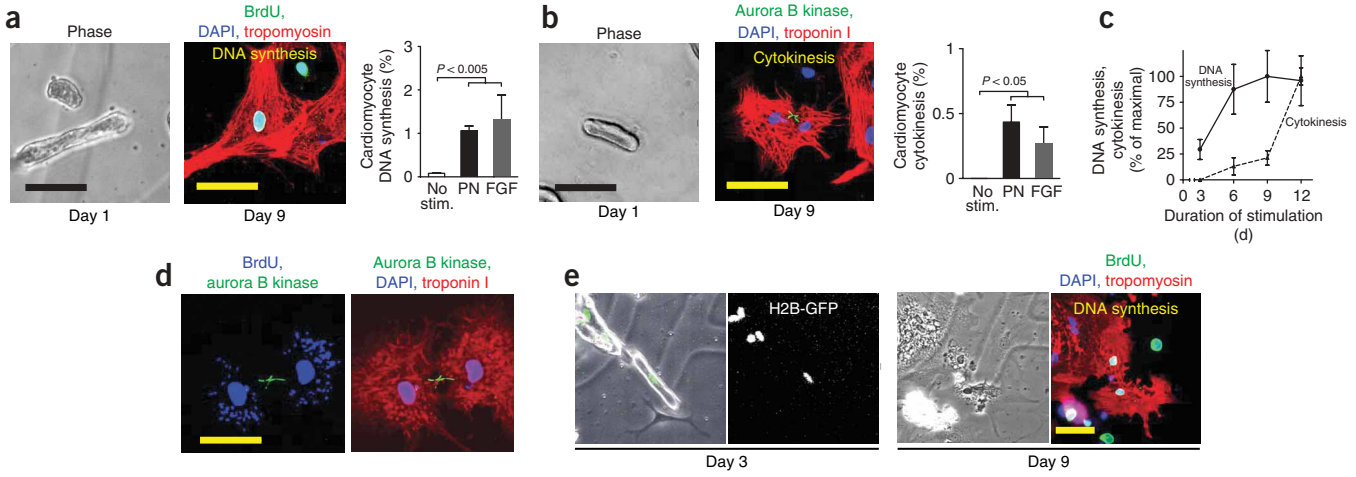

Figure 1 Periostin stimulates DNA synthesis and cytokinesis of differentiated mononucleated cardiomyocytes. (**a**,**b**) Primary adult rat ventricular cardiomyocytes were photographed in phase contrast after attachment; they were then stimulated with periostin, labeled with BrdU for the last 3 d, and cell cycle activity was determined by immunofluorescence microscopy after 9 days. Examples of corresponding phase contrast images (left micrographs) and immunofluorescent images (right micrographs) and results of quantification are shown. (**a**) Cardiomyocyte in S phase retaining expression of tropomyosin. (**b**) Cardiomyocyte in cytokinesis expressing troponin I. (**c**) Cardiomyocytes were stimulated with periostin, BrdU was added for the last 3 d, and DNA synthesis and cytokinesis were analyzed at the indicated times. (**d**) BrdU-labeled cardiomyocyte in cytokinesis. (**e**) Cardiomyocyte nuclei visualized by troponin T–controlled expression of H2B-GFP. DNA synthesis was visualized 9 d after addition of BrdU for the last 3 d. Color codes for antibody staining are indicated. Scale bars, 50 μm. No stim., no stimulation; PN, periostin. Data are mean ± s.e.m. of 8 (**a**), 6 (**b**) and 3 (**c**) experiments. Statistical significance was tested by ANOVA.

increase in cardiomyocyte DNA synthesis to 1.1 ± 0.2%, similar to the effect of fibroblast growth factor (FGF), which is known to promote cell-cycle reentry of differentiated cardiomyocytes[4] (**Fig. 1a**).

We detected cytokinesis, the final step of the mitotic cell cycle, by visualizing aurora B kinase, a component of the contractile ring at the site of cytoplasmic separation that is required for cytokinesis[19]. Non-stimulated cardiomyocytes did not progress into cytokinesis. In cardiomyocytes stimulated with periostin, aurora B kinase was detected after dissociation from the midbody, characteristic of the completion of cytokinesis (**Fig. 1b**). Periostin stimulated cytokinesis in 0.5 ± 0.2% of cardiomyocytes, similar to the effect of FGF (**Fig. 1b**).

Because most adult mammalian cardiomyocytes are binucleated[20], a possible origin of cardiomyocyte cytokinesis is breakdown of binucleated cardiomyocytes into mononucleated cardiomyocytes, without prior DNA synthesis. Periostin-induced cardiomyocyte DNA synthesis began after 3 d; however, cytokinesis was not detected before 6 d (**Fig. 1c**). If periostin-stimulated DNA synthesis preceded cytokinesis, then cardiomyocytes in cytokinesis should be positive for BrdU. We detected BrdU-labeled nuclei in 100% of cardiomyocyte cytokineses ($n = 58$; **Fig. 1d**). Using a third-generation lentivirus[21], we genetically labeled autologous cardiac fibroblasts to exclude the possibility that their fusion with differentiated cardiomyocytes induced cell-cycle reentry (**Supplementary Fig. 2** online). In conclusion, periostin induces the full mitotic cell cycle in differentiated cardiomyocytes.

Hoechst 33342 staining showed that 7.3 ± 1.7% ($n = 6$) of rod-shaped cardiomyocytes were mononucleated, consistent with other reports[20,22,23]. To test whether mono- and binucleated cardiomyocytes have the same proliferative potential, we visualized the expression of nuclear histone-2B tagged with green fluorescent protein (H2B-GFP; **Fig. 1e**, left) and analyzed cell-cycle activity after 6 d (**Fig. 1e**, right). After 3 d of BrdU labeling, 1.7 ± 0.3% of all mononucleated cardiomyocytes were BrdU positive. By contrast, only 0.2 ± 0.03% of binucleated cardiomyocytes were BrdU positive ($P \leq 0.001$). Thus, differentiated mononucleated cardiomyocytes have higher proliferative potential than do binucleated cardiomyocytes.

Cardiomyocyte cycling requires integrins and PI3K

Periostin-induced cardiomyocyte cell-cycle reentry was concentration-dependent (**Supplementary Fig. 3** online) and did not correlate with the abundance of cardiac fibroblasts (**Supplementary Fig. 4** online), suggesting that periostin has a direct effect on cardiomyocytes. Integrins may function as periostin receptors in cardiomyocytes[10]. We therefore determined whether blocking specific integrin subunits would inhibit periostin-stimulated cardiomyocyte cell-cycle activity. Antibodies specific to α_V, β_1, β_3 and β_5 integrins inhibited periostin-stimulated DNA synthesis in differentiated cardiomyocytes, whereas blocking α_7 integrin had no effect (**Fig. 2a**). Reducing the expression of integrin α_V or β_1 by RNA-mediated interference (RNAi) inhibited periostin-induced cell-cycle reentry in neonatal cardiomyocytes (**Supplementary Fig. 5** online). We conclude that periostin requires integrin α_V and a β_1, β_3 or β_5 subunit to induce cardiomyocyte cell-cycle reentry.

FGF-induced cardiomyocyte cell-cycle reentry is enhanced by concurrently inhibiting p38 mitogen-activated protein (MAP) kinase[4]. We therefore determined whether periostin-induced cardiomyocyte cell-cycle reentry could be augmented by adding FGF (100 ng/ml) or by inhibiting p38 MAP kinase with the compound SB203580 (5 μM). Whereas adding FGF increased periostin-induced cardiomyocyte DNA synthesis, inhibiting p38 MAP kinase had no additional effect (**Fig. 2b**).

Integrins activate the extracellular signal–regulated kinases 1 and 2 (ERK1/2) and PI3K pathways of the MAP kinase cascade[24]. In neonatal cardiomyocytes, compounds blocking the ERK1/2 pathway did not inhibit periostin-induced cell-cycle reentry (**Supplementary Fig. 6** online). In differentiated cardiomyocytes, blocking the ERK1/2 pathway with the compounds PD98059 (1 μM) and U0126 (10 μM) did not reduce periostin-induced cell-cycle reentry, whereas under the same conditions they inhibited neuregulin-induced cell-cycle reentry (**Fig. 2c**). These results indicate that the ERK1/2 pathway is not required for periostin-induced cell-cycle reentry of differentiated cardiomyocytes. LY294002 (10 μM) fully inhibited periostin-induced

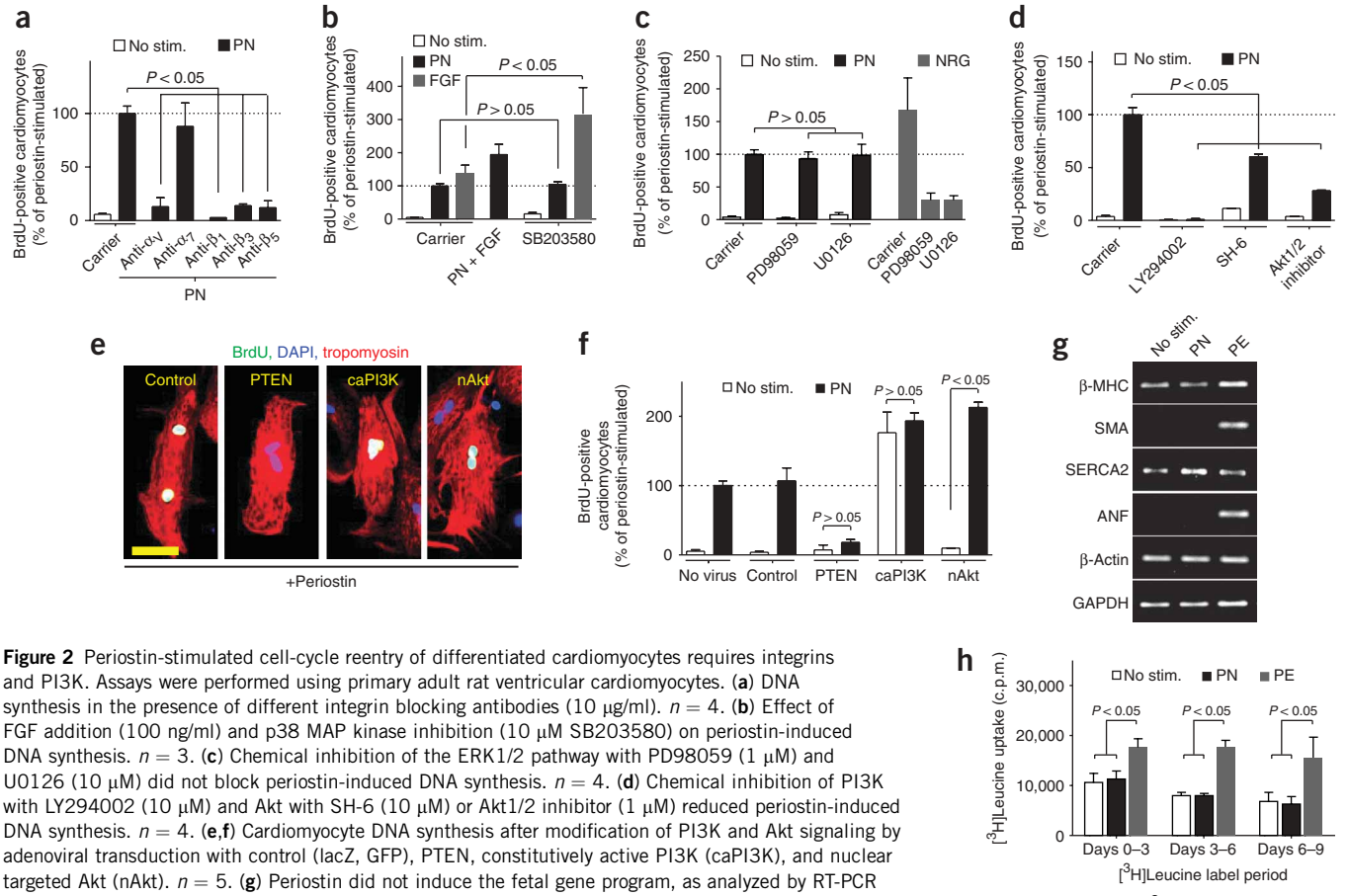

Figure 2 Periostin-stimulated cell-cycle reentry of differentiated cardiomyocytes requires integrins and PI3K. Assays were performed using primary adult rat ventricular cardiomyocytes. (**a**) DNA synthesis in the presence of different integrin blocking antibodies (10 μg/ml). $n = 4$. (**b**) Effect of FGF addition (100 ng/ml) and p38 MAP kinase inhibition (10 μM SB203580) on periostin-induced DNA synthesis. $n = 3$. (**c**) Chemical inhibition of the ERK1/2 pathway with PD98059 (1 μM) and U0126 (10 μM) did not block periostin-induced DNA synthesis. $n = 4$. (**d**) Chemical inhibition of PI3K with LY294002 (10 μM) and Akt with SH-6 (10 μM) or Akt1/2 inhibitor (1 μM) reduced periostin-induced DNA synthesis. $n = 4$. (**e**,**f**) Cardiomyocyte DNA synthesis after modification of PI3K and Akt signaling by adenoviral transduction with control (lacZ, GFP), PTEN, constitutively active PI3K (caPI3K), and nuclear targeted Akt (nAkt). $n = 5$. (**g**) Periostin did not induce the fetal gene program, as analyzed by RT-PCR 4 d after stimulation. Representative example of three repeat experiments. (**h**) Periostin did not induce hypertrophy, as determined by [^{3}H]leucine uptake. $n = 3$. Scale bar, 50 μm. PN, periostin; NRG, neuregulin-1β; PE, phenylephrine; GAPDH, glyceraldehyde 3-phosphate dehydrogenase.

cardiomyocyte cell-cycle reentry, however, suggesting that the PI3K pathway may be involved (**Fig. 2d**). The protein kinase Akt is an important downstream target of PI3K in cardiomyocytes[25]. Inhibition of Akt signaling with two different compounds, SH-6 (10 μM) or an Akt1/2 inhibitor (1 μM), reduced periostin-induced cardiomyocyte cell-cycle reentry (**Fig. 2d**).

To confirm these results, we used adenoviral transduction to express regulators of the PI3K pathway. Activation of the PI3K cascade was functionally disrupted by transducing the bifunctional phosphatase PTEN[26]. Expression of PTEN abolished periostin-stimulated DNA synthesis in cardiomyocytes (**Fig. 2e**,**f**), indicating that periostin releases the proliferative potential of differentiated cardiomyocytes in a PI3K-dependent mechanism. Transduction of a constitutively active form of PI3K[27] increased cardiomyocyte DNA synthesis in the absence of periostin (**Fig. 2f**), and adding periostin did not further augment cardiomyocyte cell-cycle reentry (**Fig. 2f**). Cardiomyocyte cell-cycle reentry induced by constitutively active PI3K was associated with abnormally shaped nuclei (**Fig. 2e**). Whereas constitutively active Akt induces cardiomyocyte hypertrophy[25], nuclear targeted Akt is associated with cardiomyocyte proliferation[28]. Accordingly, we transduced nuclear targeted Akt, which had no effect on cardiomyocyte DNA synthesis in the absence of periostin. In the presence of periostin, nuclear targeted Akt doubled the proportion of DNA-synthesizing cardiomyocytes (**Fig. 2f**). Taken together, these results suggest that PI3K signaling is required for periostin-induced reentry of differentiated cardiomyocytes into the cell cycle and is sufficient for cell-cycle reentry in the absence of periostin.

The PI3K pathway is associated with cardiomyocyte hypertrophy and apoptosis[25]. We tested whether periostin induces hypertrophy of differentiated cardiomyocytes. Transcription of β-myosin heavy chain (β-MHC), smooth muscle actin (SMA) and atrial natriuretic factor (ANF), markers of the fetal gene program induced in hypertrophy, was not increased by periostin in adult ventricular cardiomyocytes (**Fig. 2g**). By contrast, positive control samples treated with phenylephrine showed increased transcription of β-MHC, SMA and ANF. Transcription of the sarco-/endoplasmic reticulum Ca^{2+}-ATPase (SERCA2) was slightly increased in periostin-treated samples and slightly reduced in phenylephrine-treated positive controls, consistent with decreased SERCA2 transcription in hypertrophy[29]. These results indicate that periostin does not induce the fetal gene program.

Induction of the fetal gene program is accompanied by increased protein synthesis leading to cardiomyocyte hypertrophy. We assessed cardiomyocyte hypertrophy by measuring uptake of [^{3}H]leucine. Whereas the positive control phenylephrine (10 μM) induced [^{3}H]leucine uptake, periostin did not induce uptake at any of the time points tested (**Fig. 2h**). In addition, periostin did not reduce doxorubicin or TNF-α-induced cardiomyocyte death (**Supplementary Fig. 6**).

Periostin stimulates cardiomyocyte cycling *in vivo*

To test whether periostin stimulates cardiomyocyte cell cycle reentry *in vivo*, recombinant periostin was injected into the myocardium. The presence of injected periostin was confirmed by immunofluorescence microscopy (**Fig. 3a**). Recombinant periostin did not induce fibrosis

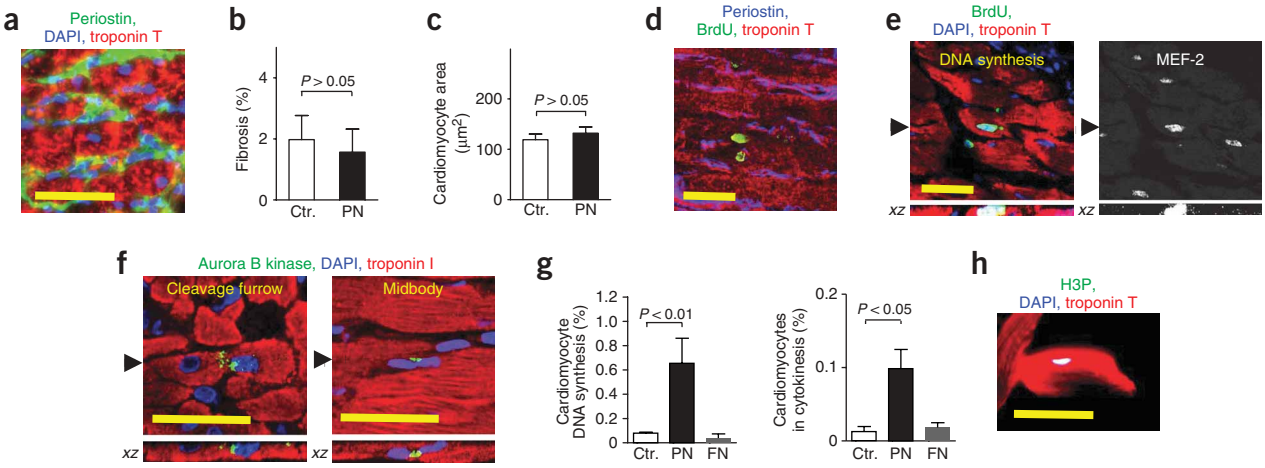

Figure 3 Periostin stimulates cardiomyocyte DNA synthesis and cytokinesis *in vivo*. Buffer, periostin or fibronectin were injected into the myocardium of rats. Cardiomyocyte cell-cycle reentry was determined after three injections of BrdU over 7 d. (**a**) The presence of periostin in injected hearts was confirmed by immunofluorescence microscopy. (**b**,**c**) Digital quantification of fibrosis (**b**) and cardiomyocyte cross-sectional area (**c**). (**d**) An example of a BrdU-positive cardiomyocyte nucleus adjacent to injected periostin. (**e**) Cardiomyocyte DNA synthesis in periostin-treated hearts and expression of the myogenic marker MEF-2. (**f**) Cytokinesis as determined by visualization of cleavage furrow and midbody with aurora B kinase immunofluorescence. Arrowheads indicate reconstructed *xz* planes shown below (**e**,**f**). (**g**) Quantification of cardiomyocyte DNA synthesis and cytokinesis. (**h**) H3P-positive mononucleated differentiated cardiomyocyte. Color codes for antibody staining are indicated. Scale bars, 50 μm. Ctr., buffer (3 rats); PN, periostin (4 rats); FN, fibronectin (5 rats). Statistical significance was tested by *t*-test.

(**Fig. 3b**) or hypertrophy (**Fig. 3c**). Three intraperitoneal injections of BrdU with a half-life of 2 h (ref. 30) were administered to detect a portion of cycling cardiomyocytes. After 7 d, cycling cardiomyocytes were present near the injected areas (**Fig. 3d**). BrdU-positive cardiomyocytes had a differentiated phenotype, as indicated by striations, expression of contractile protein (troponin T), and expression of the myogenic transcription factor MEF-2 (**Fig. 3e**). Reconstruction of optical sections enabled us to assign BrdU-positive nuclei unequivocally to cardiomyocytes (**Fig. 3e**, bottom). We determined whether periostin stimulates cardiomyocyte division *in vivo*. By visualizing the cleavage furrow and the midbody, we detected differentiated cardiomyocytes during (**Fig. 3f**, left) and after (**Fig. 3f**, right) cytokinesis. Reconstruction of optical sections provided unequivocal assignment of cleavage furrows and midbodies to dividing cardiomyocytes (**Fig. 3f**, bottom). Periostin induced DNA synthesis in 0.7 ± 0.1% and cytokinesis in 0.1 ± 0.03% of cardiomyocyte nuclei in the injected area (**Fig. 3g**). To confirm that cardiomyocyte proliferation is a specific effect of periostin and not a response to nonspecific changes in the extracellular matrix, fibronectin was injected into control hearts. Fibronectin did not increase cardiomyocyte DNA synthesis or cytokinesis (**Fig. 3g**). These results indicate that periostin induces DNA synthesis and division of differentiated cardiomyocytes *in vivo*.

We determined whether mononucleated cardiomyocytes are more likely to reenter the cell-cycle *in vivo* by visualizing cycling cardiomyocyte nuclei with an antibody specific to phosphorylated histone H3 (H3P) on dispersed isolated cardiomyocytes (**Fig. 3h**). Whereas 2 ± 0.2% of mononucleated cardiomyocytes were H3P positive, only 0.04 ± 0.01% of binucleated cardiomyocytes were H3P positive ($P = 0.0005$), consistent with the *in vitro* findings.

Periostin improves cardiac function after myocardial infarction

Sustained cardiomyocyte cell-cycle activity may improve function and decrease infarct size after myocardial infarction[6,7,31,32]. To develop a long-term delivery system, we determined the ability of periostin to associate with Gelfoam, a biodegradable extracellular matrix preparation. Periostin bound to Gelfoam and was gradually released (**Fig. 4a**). At the time of myocardial infarction, we administered epicardial Gelfoam patches loaded with periostin or with buffer and determined the presence of recombinant periostin in the left ventricle after 12 weeks. The distance from the epicardium to the farthest diffusion range of periostin was 461 ± 62 μm (**Fig. 4b**). We confirmed the presence of periostin in the left ventricle by immunoblotting (**Fig. 4c**). To determine whether delivery of recombinant periostin improves cardiac function, echocardiography was performed 1 and 12 weeks after myocardial infarction (**Fig. 4d**,**e**). Between 1 and 12 weeks, the shortening fraction in periostin-treated rats increased from 25 to 33% and the ejection fraction increased from 53 to 66% (**Fig. 4d**,**e** and **Supplementary Table 1**). In control rats, by contrast, the shortening and ejection fractions were unchanged.

We analyzed post-infarction ventricular remodeling by echocardiography. At 1 week after myocardial infarction, the treatment and control groups had the same end-diastolic dimension (**Supplementary Table 1**). At 12 weeks, however, the left ventricular end-diastolic dimension was significantly smaller in periostin-treated rats, suggesting improved ventricular remodeling (**Supplementary Table 1**).

We obtained a second measure of cardiac function 12 weeks after myocardial infarction by catheterization of the left ventricle during preload reduction (**Fig. 4f**,**g**). Treatment with periostin improved myocardial function, as indicated by a steeper slope of the end-systolic pressure-volume relationship, a higher preload recruitable stroke work, a higher maximum rate of ventricular pressure rise, and a higher maximum ventricular elastance (**Fig. 4f**,**g**, and **Supplementary Table 1**). Thus, myocardial delivery of periostin improves ventricular remodeling and cardiac function after myocardial infarction.

Periostin reduces fibrosis and hypertrophy

To determine how periostin improves cardiac function, we compared the structure of control and periostin-treated hearts at 1 and 12 weeks after myocardial infarction. Periostin-treated and control hearts had

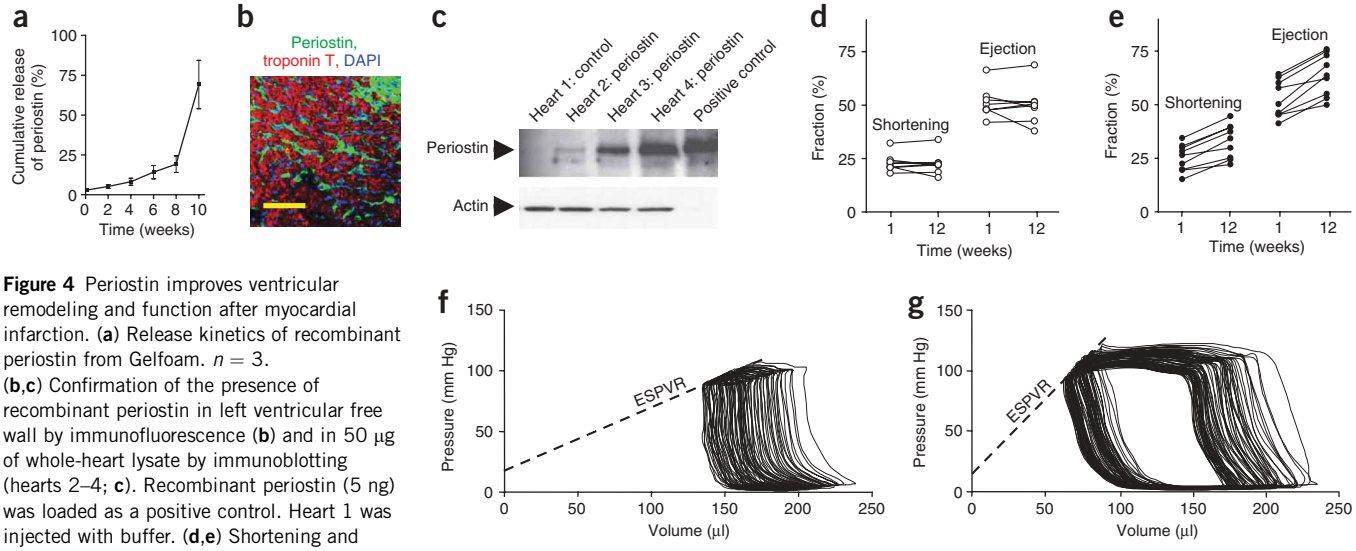

Figure 4 Periostin improves ventricular remodeling and function after myocardial infarction. (**a**) Release kinetics of recombinant periostin from Gelfoam. $n = 3$. (**b**,**c**) Confirmation of the presence of recombinant periostin in left ventricular free wall by immunofluorescence (**b**) and in 50 μg of whole-heart lysate by immunoblotting (hearts 2–4; **c**). Recombinant periostin (5 ng) was loaded as a positive control. Heart 1 was injected with buffer. (**d**,**e**) Shortening and ejection fractions after 1 and 12 weeks of administration of control buffer (**d**) or recombinant periostin (**e**). (**f**,**g**) Representative left ventricular pressure-volume loops obtained after 12 weeks of administration of control buffer (**f**) or periostin (**g**). End-systolic pressure-volume relationship (ESPVR) during preload reduction is indicated by the dashed line. Scale bar, 50 μm (**b**).

the same infarct size 1 week after myocardial infarction (**Fig. 5a–c**). At 12 weeks after myocardial infarction, by contrast, periostin-treated hearts had a smaller scar volume (**Fig. 5c**). Because genetic deletion of β_1 or β_3 integrin induces cardiac fibrosis[33,34], we tested whether application of periostin, a ligand of β_1 and β_3 integrins, reduces scar formation. The number of BrdU-positive cardiac fibroblasts was decreased in periostin-treated hearts 1 week after myocardial infarction (**Fig. 5d**), consistent with the decrease in fibrosis determined 12 weeks after myocardial infarction (**Fig. 5e**).

We analyzed ventricular remodeling by measuring the thickness of the left ventricular free wall and the interventricular septum 12 weeks after myocardial infarction. The left ventricular free wall was thicker and the septum was thinner in periostin-treated hearts (**Fig. 5f**), consistent with improved remodeling. We also analyzed cardiac hypertrophy, a component of ventricular remodeling. Despite the smaller infarct size in periostin-treated rats 12 weeks after myocardial infarction, heart weight was similar to that in buffer-treated rats (**Fig. 5g**). By contrast, periostin-treated rats had a smaller cross-sectional cardiomyocyte area than did control rats, indicating less cellular hypertrophy (**Fig. 5h**). These results indicate that sustained administration of recombinant periostin reduces infarct size and improves ventricular remodeling.

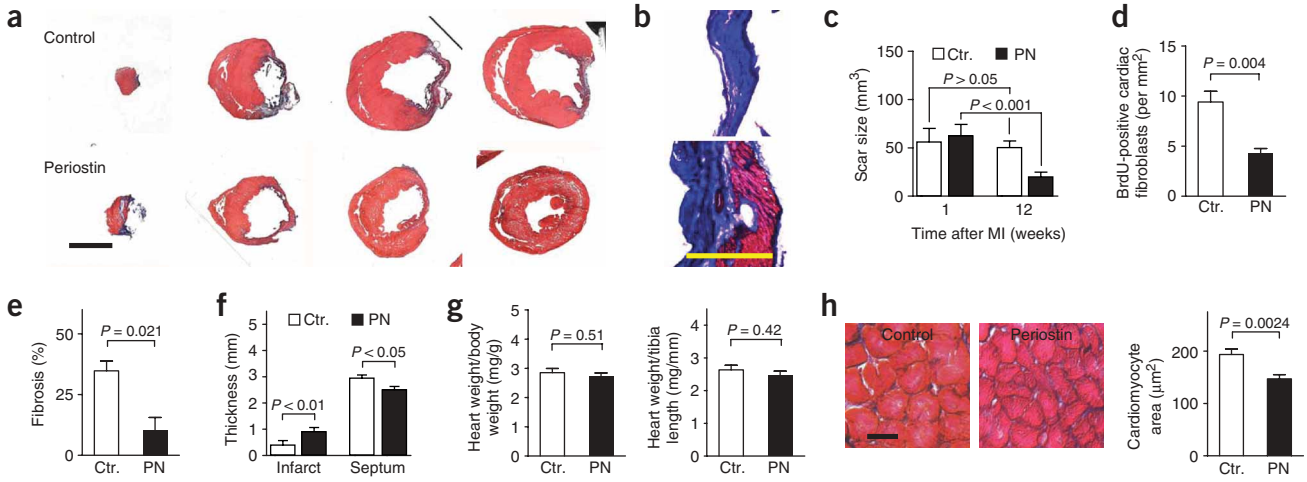

Figure 5 Periostin reduces scar formation and attenuates post-infarct remodeling. Rats with experimental myocardial infarction (MI) were treated with control Gelfoam or periostin Gelfoam and analyzed after 1 or 12 weeks. (**a–c**) Visualization (**a**,**b**) and quantification (**c**) of infarct scar size after 12 weeks of administration of buffer (control, top panels in **a**,**b**) or periostin (lower panels in **a**,**b**). (**d**) Number of proliferating cardiac fibroblasts 1 week after myocardial infarction. (**e**) Determination of fibrosis at 12 weeks. (**f**) Analysis of cardiac remodeling by quantification of the thickness of ventricular wall in infarct area and septum. (**g**) Analysis of heart organ hypertrophy 12 weeks after myocardial infarction by heart/body weight ratio and heart weight/tibia length ratio. (**h**) Analysis of cardiomyocyte hypertrophy by cross-sectional area. Scale bars, 5 mm (**a**); 0.5 mm (**b**); 50 μm (**h**). Statistical significance was tested by *t*-test (**d**,**e**,**g**,**h**) and ANOVA (**c**,**f**). Ctr., control hearts receiving Gelfoam with buffer ($n = 12$); PN, hearts receiving Gelfoam with periostin ($n = 18$).

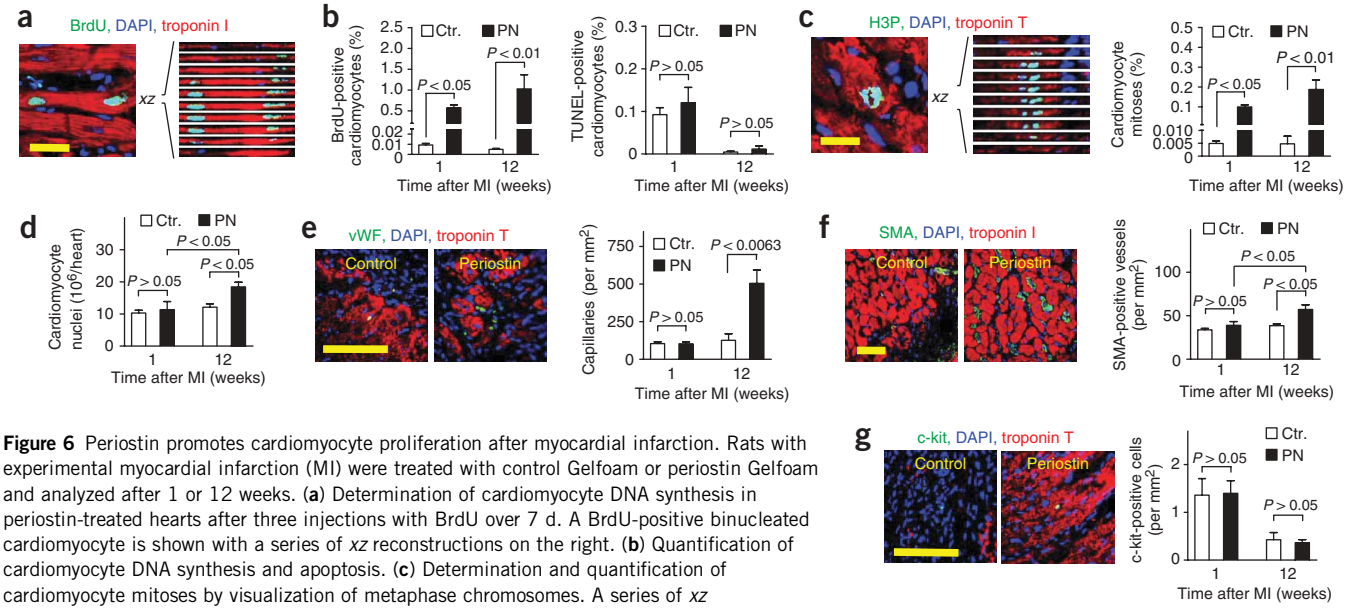

Figure 6 Periostin promotes cardiomyocyte proliferation after myocardial infarction. Rats with experimental myocardial infarction (MI) were treated with control Gelfoam or periostin Gelfoam and analyzed after 1 or 12 weeks. (**a**) Determination of cardiomyocyte DNA synthesis in periostin-treated hearts after three injections with BrdU over 7 d. A BrdU-positive binucleated cardiomyocyte is shown with a series of *xz* reconstructions on the right. (**b**) Quantification of cardiomyocyte DNA synthesis and apoptosis. (**c**) Determination and quantification of cardiomyocyte mitoses by visualization of metaphase chromosomes. A series of *xz* reconstructions is shown to the right of the micrograph. (**d**) Quantification of left ventricular cardiomyocyte nuclei. (**e**) Capillary density determined with antibody to von Willebrand factor (vWF). (**f**) Arteriolar density determined with antibody to SMA. (**g**) Quantification of c-kit-positive stem cells in infarct area and border zone. Scale bars, 50 μm. Ctr., control rats receiving Gelfoam with buffer ($n = 12$); PN, rats receiving Gelfoam with periostin ($n = 18$). Statistical significance was tested by ANOVA.

Periostin enhances cardiac repair

How does periostin reduce infarct size? The *in vitro* results pointed to cardiomyocyte proliferation as a possible mechanism. To determine whether the decrease in infarct size correlated with cardiomyocyte cell-cycle reentry, we quantified DNA synthesis in the infarct and border zone at 1 and 12 weeks after myocardial infarction. Cardiomyocytes were identified by expression of the cardiac contractile protein troponin I and by their characteristic shape (**Fig. 6a**). Treatment with periostin induced BrdU uptake in 0.6 ± 0.07% of cardiomyocytes at 1 week and in 1 ± 0.3% at 12 weeks (**Fig. 6b**). The proportion of apoptotic cardiomyocytes was similar in control and periostin-treated hearts at both 1 and 12 weeks (**Fig. 6b**). In periostin-treated hearts, however, the proportion of cycling cardiomyocytes was fivefold higher than the proportion of apoptotic cardiomyocytes at 1 week after myocardial infarction and 100-fold higher at 12 weeks (**Fig. 6b**), suggesting that proliferation of differentiated cardiomyocytes may be the cellular mechanism underlying the decrease in infarct size in periostin-treated hearts. We investigated this possibility by visualizing H3P in condensed metaphase chromosomes in differentiated cardiomyocytes during mitosis (**Fig. 6c**). Treatment with periostin induced mitosis in 0.1 ± 0.01% of cardiomyocyte nuclei at 1 week and in 0.2 ± 0.5% at 12 weeks (**Fig. 6c**).

Can these proliferating indices account for the observed functional improvement? After a single injection of BrdU, providing effective labeling for 6.4 h (ref. 30), we determined cell-cycle reentry of 23,852 ± 1,709 differentiated cardiomyocytes per heart ($n = 3$). The resulting rate of 3,727 cardiomyocytes entering the cell cycle per hour is calculated to result in 7.2×10^6 new cardiomyocyte nuclei per heart after 12 weeks. By quantifying cardiomyocytes with metaphase chromosomes, we independently determined 4,737 ± 770 ($n = 6$) cardiomyocyte mitoses in periostin-treated hearts. Chromosome condensation persisted for 1.7 ± 0.4 h as determined by time-lapse video microscopy. This rate of cardiomyocyte mitosis is calculated to result in the generation of 5.5×10^6 cardiomyocyte nuclei over a period of 12 weeks. We also quantified cardiomyocyte nuclei directly. At 1 week after myocardial infarction, control and periostin-treated hearts had the same number of nuclei (**Fig. 6d**). At 12 weeks after myocardial infarction, by contrast, periostin-treated hearts had 6.2×10^6 more cardiomyocyte nuclei than did control hearts (**Fig. 6d**), consistent with the results based on proliferative indices. Cell-cycle reentry and division of differentiated cardiomyocytes can therefore account for the periostin-induced functional and structural improvements.

To determine whether periostin stimulates angiogenesis after myocardial infarction, we quantified the density of capillaries and arterioles in the region of the infarct and in the border zone. At 1 week, the capillary (**Fig. 6e**) and arteriolar (**Fig. 6f**) densities did not differ between control and periostin-treated hearts. At 12 weeks after myocardial infarction, however, periostin-treated hearts had a 4-fold increase in capillary and a 1.5-fold increase in arteriolar density as compared with control hearts. Improved cardiac function is associated with recruitment of c-kit-positive stem cells[35]. However, the number of c-kit-positive cells in the infarct and border zone did not differ between periostin-treated and control hearts at 1 and at 12 weeks after myocardial infarction (**Fig. 6g**).

DISCUSSION

Increased cardiomyocyte DNA synthesis in the border zone of a myocardial infarction suggests that some differentiated cardiomyocytes reenter the cell cycle[1]. Our results show that differentiated mononucleated cardiomyocytes have proliferative potential. We have demonstrated that, after myocardial infarction, periostin-induced cycling of differentiated cardiomyocytes is associated with improved myocardial function and remodeling and with infarct regression.

We have shown that, to induce cardiomyocyte proliferation, periostin requires α_V and an β_1, β_3 or β_5 integrin subunit, consistent with results from other systems[9]. Integrins are upregulated in the infarct border zone[36] but have not been implicated in cell-cycle reentry of differentiated cardiomyocytes. Cardiac-specific knockout of β_1 (ref. 33) or β_3 (ref. 34) integrin results in increased fibrosis; this is consistent with our finding that periostin, a ligand of β_1 and β_3

integrins, markedly decreases fibrosis after myocardial infarction, and is also consistent with the increased extracellular matrix deposition in the heart valves of periostin knockout mice[37].

Recombinant extracellular periostin did not induce cardiomyopathy. This finding contrasts with two previous studies of cardiac overexpression of periostin or periostin-like factor. Liposomal gene delivery of periostin was found to cause dilated cardiomyopathy without hypertrophy[17], whereas adenoviral gene delivery of periostin-like factor induced hypertrophy[16]. This apparent discrepancy may be due to the fact that cardiac fibroblasts usually express periostin and secrete it into the extracellular matrix[12], whereas delivery by gene transfer results in significant intracellular retention[38,39].

The lower wall stress in periostin-treated hearts determined by catheterization decreased the hypertrophic drive after myocardial infarction, consistent with the smaller cardiomyocyte cross-sectional area observed. This finding suggests that sustained cardiomyocyte replacement may have attenuated the increase in wall stress after myocardial infarction, resulting in improved ventricular remodeling. Administration of periostin induced cell-cycle reentry in 0.6–1% of all cardiomyocytes in the infarct border zone without affecting apoptosis. This proportion of cycling cardiomyocytes is comparable to that observed for cyclin D2 transgenes, for combined p53 and p193 dominant-negative transgenes, after gene therapy with cyclin A2, and after administration of FGF coupled with a p38 MAP kinase block[6,7,31,32] (**Supplementary Table 2** online).

The PI3K/Akt pathway controls cell size, including cardiomyocyte size[40]. We found that periostin, like FGF[4], requires the PI3K/Akt pathway to induce cardiomyocyte cell-cycle reentry. Because of the myocardial protective effect of Akt[27], it is tempting to propose that periostin has an antiapoptotic effect. However, our data show that periostin has no protective effect, suggesting that the proapoptotic signals dominate over possible protection through periostin-induced PI3K activation. After myocardial infarction, the epicardial delivery strategy may not effectively reach all cardiomyocytes in the ischemic area to induce functionally and structurally relevant myocardial protection.

Improvement of myocardial function can be achieved with circulating or resident stem cells, which requires their isolation, *in vitro* propagation, and transplantation[41]. Although our results do not exclude the possibility that cardiogenic stem cells contribute to periostin-induced myocardial repair, we have shown that a subpopulation of differentiated cardiomyocytes has proliferative potential. Stimulating proliferation of endogenous cardiomyocytes with periostin, periostin derivatives, or mimetics may provide an innovative approach to induce myocardial repair.

METHODS

Cardiomyocyte isolation and culture. Experiments were approved by the Animal Care and Use Committee of Children's Hospital Boston. Primary adult ventricular cardiomyocytes were isolated from male (300 g) Wistar rats (Charles River Laboratories) and maintained as described[4]. We added periostin (500 ng/ml; BioVendor), FGF (100 ng/ml; R&D Systems), neuregulin-1β (NRG, 100 ng/ml; R&D Systems), or phenylephrine (10 μM; Sigma) every 3 d for 9 d, and 30 μM BrdU for the last 3 d. Inhibitory antibodies were added at a concentration of 10 μg/ml, cyclic arginine-glycine-aspartate (cRGD) at 10 μM, SB203580 at 5 μM, U0126 at 10 μM, PD98059 at 1 μM, LY294002 at 10 μM, SH-6 at 10 μM, and Akt1/2 inhibitor at 1 μM 30 min before stimulation. The vehicle used to dissolve factors or chemicals was added to unstimulated samples, which were then processed together with the test samples.

Immunofluorescence microscopy. Binding of primary antibodies (see **Supplementary Methods** online) was visualized with fluorophore-conjugated secondary antibodies (Invitrogen). We visualized nuclei with 4′,6′-diamidino-2-phenylindole (DAPI; Invitrogen). For image acquisition, the γ value was set at 1 and the lookup table settings were linear (see **Supplementary Table 3** online).

Determination of cardiomyocyte ploidy. Cardiomyocytes were incubated with 0.2 μg/ml of Hoechst 33342 (Invitrogen) for 10 min. We counted nuclei in four random ×20 microscopic fields.

Cardiomyocyte fate tracking. Cardiomyocytes were grown on gridded coverslips (Electron Microscopy Services) and imaged in phase contrast at ×10 magnification. Cardiomyocytes were transduced with an adenovirus leading to nuclear expression of H2B-GFP[42] under control of the chicken troponin T promoter[43]. Imaging and infection conditions did not affect cell proliferation or viability (data not shown). We matched images of BrdU-positive cardiomyocytes with corresponding images taken before stimulation. For quantification, differentiated cardiomyocytes were defined as striated rod-shaped structures with a length to width ratio of >1.5.

Gene transfer. We generated type-5 recombinant adenoviruses as described[44]. Constitutively active PI3K[27], nuclear Akt[45] and PTEN were expressed under control of the cytomegalovirus (CMV) promoter. Adult rat ventricular cardiomyocytes were transduced at a multiplicity of infection of 20.

Transcriptional analysis. We stimulated cardiomyocytes for 4 d and prepared RNA by using Trizol reagent (Invitrogen). Complementary DNA synthesis and RT-PCR analysis are described in **Supplementary Methods**.

Cardiomyocyte hypertrophy assay *in vitro*. We seeded 25,000 primary adult rat ventricular cardiomyocytes in 24-well plates and labeled them with 1 μCi/well of [^{3}H]leucine for 3 d in the presence of buffer, 500 ng/ml of periostin, 100 ng/ml of FGF or 10 μM phenylephrine. The amount of [^{3}H]leucine incorporated was quantified as described[46].

Determination of cardiomyocyte cell-cycle activity *in vivo*. Experiments were approved by the Subcommittee on Research Animal Care of Massachusetts General Hospital. Injections and analyses were performed in a blinded manner. Adult male Sprague-Dawley rats (300 g; Charles River Laboratories) underwent thoracotomy and received intramyocardial injections of 50 μg periostin, 50 μg fibronectin or 100 μl 100 mM sodium acetate as a control (five rats per group). The survival rate for this procedure was 80%. We confirmed the presence of injected periostin by immunofluorescence microscopy using a polyclonal antibody to human periostin (Abcam). Intraperitoneal injections of BrdU (70 μmol per kilogram body weight), with a tissue half-life of 2 h (ref. 30), were given every 48 h, and rats were killed 48 h after the third injection. Cell-cycle activity was determined on horizontal sections spaced at 1-mm intervals by laser scanning immunofluorescence microscopy as described in **Supplementary Methods**.

Determination of release kinetics of periostin from Gelfoam. To develop a long-term delivery system for recombinant periostin, we determined whether recombinant periostin associated with Gelfoam, a biodegradable biological scaffold. Gelfoam patches (Pfizer) of 1-cm diameter were loaded with 100 μg of recombinant human periostin and incubated with 1 ml of PBS at 37 °C with continuous agitation for 10 weeks. The supernatant was replaced every 2 weeks and the concentration of recombinant periostin in the supernatant was determined by immunoblotting using a polyclonal antibody to human periostin (Abcam). We determined the diffusion range of recombinant periostin in myocardium by immunofluorescence microscopy using a polyclonal antibody to human periostin. The presence of periostin in the myocardium was determined by immunoblotting using a polyclonal antibody to human periostin (Abcam).

Rat model of myocardial infarction and analysis of myocardial regeneration. Adult male Sprague-Dawley rats (300 g; Charles River Laboratories) underwent experimental myocardial infarction as described[47]. The survival rate was 67%. Gelfoam loaded with either 100 μg of recombinant periostin or buffer was applied over the myocardial infarction at the time of surgery. Rats received three intraperitoneal BrdU injections (70 μmol/kg) with a half-life of 2 h (ref. 30) every 48 h over a period of 7 d. We carried out echocardiography and

hemodynamic catheterization as described[48]. Myocardial regeneration was analyzed as described in **Supplementary Methods**.

Statistical analysis. Observations were quantified (details in **Supplementary Table 4** online) by two investigators (B.K. and S.A.) independently from one another and in a blinded manner. Numerical data are the mean ± s.e.m. Statistical significance was determined by using two-tailed *t*-test and analysis of variance (ANOVA). The α value was set at 0.05 for statistical significance.

Note: Supplementary information is available on the Nature Medicine website.

ACKNOWLEDGMENTS

We thank M. Dai and L.-B. Chen (Dana Farber Cancer Institute, Boston, Massachusetts, USA) for recombinant human periostin; members of the Clapham, del Monte, Hajjar, Keating, McGowan, and Pu laboratories for discussions and sharing reagents; S.P. Sardi (Children's Hospital Boston, Boston, Massachusetts, USA) for lentivirus constructs; and R. Breitbart for suggestions and critical review of the manuscript. This study was supported in part by grants from the US National Institutes of Health (R01 HL078691, HL057263, HL071763, HL080498 and HL083156 to R.J.H.; K08 HL069842 to F.d.M.; and K01 HL076659 to D.L.) and the Leducq Transatlantic Network (to R.J.H.).

AUTHOR CONTRIBUTIONS

B.K. supervised research; B.K., F.d.M., R.J.H., Y.-S.C., D.L., S.A. and M.T.K. designed experiments; B.K., F.d.M., Y.-S.C. and S.A. performed and analyzed experiments; F.d.M., Y.-S.C., and D.L. provided plasmids and adenovirus constructs; B.K. and S.A. wrote the manuscript.

COMPETING INTERESTS STATEMENT

The authors declare competing financial interests: details accompany the full-text HTML version of the paper at http://www.nature.com/naturemedicine/.

Published online at http://www.nature.com/naturemedicine
Reprints and permissions information is available online at http://npg.nature.com/reprintsandpermissions

1. Soonpaa, M.H. & Field, L.J. Survey of studies examining mammalian cardiomyocyte DNA synthesis. *Circ. Res.* **83**, 15–26 (1998).
2. Laflamme, M.A. & Murry, C.E. Regenerating the heart. *Nat. Biotechnol.* **23**, 845–856 (2005).
3. Pasumarthi, K.B. & Field, L.J. Cardiomyocyte cell cycle regulation. *Circ. Res.* **90**, 1044–1054 (2002).
4. Engel, F.B. *et al.* p38 MAP kinase inhibition enables proliferation of adult mammalian cardiomyocytes. *Genes Dev.* **19**, 1175–1187 (2005).
5. Katz, E.B. *et al.* Cardiomyocyte proliferation in mice expressing α-cardiac myosin heavy chain-SV40 T-antigen transgenes. *Am. J. Physiol.* **262**, H1867–H1876 (1992).
6. Pasumarthi, K.B., Nakajima, H., Nakajima, H.O., Soonpaa, M.H. & Field, L.J. Targeted expression of cyclin D2 results in cardiomyocyte DNA synthesis and infarct regression in transgenic mice. *Circ. Res.* **96**, 110–118 (2005).
7. Nakajima, H., Nakajima, H.O., Tsai, S.C. & Field, L.J. Expression of mutant p193 and p53 permits cardiomyocyte cell cycle reentry after myocardial infarction in transgenic mice. *Circ. Res.* **94**, 1606–1614 (2004).
8. Takeshita, S., Kikuno, R., Tezuka, K. & Amann, E. Osteoblast-specific factor 2: cloning of a putative bone adhesion protein with homology with the insect protein fasciclin I. *Biochem. J.* **294**, 271–278 (1993).
9. Litvin, J., Zhu, S., Norris, R. & Markwald, R. Periostin family of proteins: therapeutic targets for heart disease. *Anat. Rec. A Discov. Mol. Cell. Evol. Biol.* **287**, 1205–1212 (2005).
10. Butcher, J.T., Norris, R.A., Hoffman, S., Mjaatvedt, C.H. & Markwald, R.R. Periostin promotes atrioventricular mesenchyme matrix invasion and remodeling mediated by integrin signaling through Rho/PI 3-kinase. *Dev. Biol.* **302**, 256–266 (2007).
11. Stanton, L.W. *et al.* Altered patterns of gene expression in response to myocardial infarction. *Circ. Res.* **86**, 939–945 (2000).
12. Wang, D. *et al.* Effects of pressure overload on extracellular matrix expression in the heart of the atrial natriuretic peptide-null mouse. *Hypertension* **42**, 88–95 (2003).
13. Lindner, V., Wang, Q., Conley, B.A., Friesel, R.E. & Vary, C.P. Vascular injury induces expression of periostin: implications for vascular cell differentiation and migration. *Arterioscler. Thromb. Vasc. Biol.* **25**, 77–83 (2005).
14. Goetsch, S.C., Hawke, T.J., Gallardo, T.D., Richardson, J.A. & Garry, D.J. Transcriptional profiling and regulation of the extracellular matrix during muscle regeneration. *Physiol. Genomics* **14**, 261–271 (2003).
15. Nakazawa, T. *et al.* Gene expression of periostin in the early stage of fracture healing detected by cDNA microarray analysis. *J. Orthop. Res.* **22**, 520–525 (2004).
16. Litvin, J. *et al.* Periostin and periostin-like factor in the human heart: possible therapeutic targets. *Cardiovasc. Pathol.* **15**, 24–32 (2006).
17. Katsuragi, N. *et al.* Periostin as a novel factor responsible for ventricular dilation. *Circulation* **110**, 1806–1813 (2004).
18. Tai, I.T., Dai, M. & Chen, L.B. Periostin induction in tumor cell line explants and inhibition of in vitro cell growth by anti-periostin antibodies. *Carcinogenesis* **26**, 908–915 (2005).
19. Tatsuka, M. *et al.* Multinuclearity and increased ploidy caused by overexpression of the aurora- and Ipl1-like midbody-associated protein mitotic kinase in human cancer cells. *Cancer Res.* **58**, 4811–4816 (1998).
20. Soonpaa, M.H., Kim, K.K., Pajak, L., Franklin, M. & Field, L.J. Cardiomyocyte DNA synthesis and binucleation during murine development. *Am. J. Physiol.* **271**, H2183–H2189 (1996).
21. Rubinson, D.A. *et al.* A lentivirus-based system to functionally silence genes in primary mammalian cells, stem cells and transgenic mice by RNA interference. *Nat. Genet.* **33**, 401–406 (2003).
22. Katzberg, A.A., Farmer, B.B. & Harris, R.A. The predominance of binucleation in isolated rat heart myocytes. *Am. J. Anat.* **149**, 489–499 (1977).
23. Chen, X. *et al.* Adolescent feline heart contains a population of small, proliferative ventricular myocytes with immature physiological properties. *Circ. Res.* **100**, 536–544 (2007).
24. Miranti, C.K. & Brugge, J.S. Sensing the environment: a historical perspective on integrin signal transduction. *Nat. Cell Biol.* **4**, E83–E90 (2002).
25. Shiojima, I. & Walsh, K. Regulation of cardiac growth and coronary angiogenesis by the Akt/PKB signaling pathway. *Genes Dev.* **20**, 3347–3365 (2006).
26. Crackower, M.A. *et al.* Regulation of myocardial contractility and cell size by distinct PI3K-PTEN signaling pathways. *Cell* **110**, 737–749 (2002).
27. Matsui, T. *et al.* Adenoviral gene transfer of activated phosphatidylinositol 3′-kinase and Akt inhibits apoptosis of hypoxic cardiomyocytes in vitro. *Circulation* **100**, 2373–2379 (1999).
28. Rota, M. *et al.* Nuclear targeting of Akt enhances ventricular function and myocyte contractility. *Circ. Res.* **97**, 1332–1341 (2005).
29. Zarain-Herzberg, A., Afzal, N., Elimban, V. & Dhalla, N.S. Decreased expression of cardiac sarcoplasmic reticulum Ca^{2+}-pump ATPase in congestive heart failure due to myocardial infarction. *Mol. Cell. Biochem.* **163–164**, 285–290 (1996).
30. Gilbert, M.E., Kelly, M.E., Samsam, T.E. & Goodman, J.H. Chronic developmental lead exposure reduces neurogenesis in adult rat hippocampus but does not impair spatial learning. *Toxicol. Sci.* **86**, 365–374 (2005).
31. Woo, Y.J. *et al.* Therapeutic delivery of cyclin A2 induces myocardial regeneration and enhances cardiac function in ischemic heart failure. *Circulation* **114**, I206–I213 (2006).
32. Engel, F.B., Hsieh, P.C., Lee, R.T. & Keating, M.T. FGF1/p38 MAP kinase inhibitor therapy induces cardiomyocyte mitosis, reduces scarring, and rescues function after myocardial infarction. *Proc. Natl. Acad. Sci. USA* **103**, 15546–15551 (2006).
33. Shai, S.Y. *et al.* Cardiac myocyte-specific excision of the β_1 integrin gene results in myocardial fibrosis and cardiac failure. *Circ. Res.* **90**, 458–464 (2002).
34. Ren, J. β_3 Integrin deficiency promotes cardiac hypertrophy and inflammation. *J. Mol. Cell. Cardiol.* **42**, 367–377 (2007).
35. Fazel, S. *et al.* Cardioprotective c-kit$^+$ cells are from the bone marrow and regulate the myocardial balance of angiogenic cytokines. *J. Clin. Invest.* **116**, 1865–1877 (2006).
36. Sun, M. *et al.* Temporal response and localization of integrins β_1 and β_3 in the heart after myocardial infarction: regulation by cytokines. *Circulation* **107**, 1046–1052 (2003).
37. Rios, H. *et al.* Periostin null mice exhibit dwarfism, incisor enamel defects, and an early-onset periodontal disease-like phenotype. *Mol. Cell. Biol.* **25**, 11131–11144 (2005).
38. Yoshioka, N. *et al.* Suppression of anchorage-independent growth of human cancer cell lines by the TRIF52/periostin/OSF-2 gene. *Exp. Cell Res.* **279**, 91–99 (2002).
39. Litvin, J. *et al.* Expression and function of periostin-isoforms in bone. *J. Cell. Biochem.* **92**, 1044–1061 (2004).
40. Shioi, T. *et al.* The conserved phosphoinositide 3-kinase pathway determines heart size in mice. *EMBO J.* **19**, 2537–2548 (2000).
41. Srivastava, D. Making or breaking the heart: from lineage determination to morphogenesis. *Cell* **126**, 1037–1048 (2006).
42. Shi, Q. & King, R.W. Chromosome nondisjunction yields tetraploid rather than aneuploid cells in human cell lines. *Nature* **437**, 1038–1042 (2005).
43. Ma, H., Sumbilla, C.M., Farrance, I.K., Klein, M.G. & Inesi, G. Cell-specific expression of SERCA, the exogenous Ca^{2+} transport ATPase, in cardiac myocytes. *Am. J. Physiol. Cell Physiol.* **286**, C556–C564 (2004).
44. He, T.C. *et al.* A simplified system for generating recombinant adenoviruses. *Proc. Natl. Acad. Sci. USA* **95**, 2509–2514 (1998).
45. Shiraishi, I. *et al.* Nuclear targeting of Akt enhances kinase activity and survival of cardiomyocytes. *Circ. Res.* **94**, 884–891 (2004).
46. Lebeche, D., Kang, Z.B. & Hajjar, R. Candesartan abrogates G protein-coupled receptor agonist-induced MAPK activation and cardiac myocyte hypertrophy. *J. Renin Angiotensin Aldosterone Syst.* **2**, 154–161 (2001).
47. del Monte, F. *et al.* Abrogation of ventricular arrhythmias in a model of ischemia and reperfusion by targeting myocardial calcium cycling. *Proc. Natl. Acad. Sci. USA* **101**, 5622–5627 (2004).
48. Prunier, F. *et al.* Delayed erythropoietin therapy reduces post-MI cardiac remodeling only at a dose that mobilizes endothelial progenitor cells. *Am. J. Physiol. Heart Circ. Physiol.* **292**, H522–H529 (2007).